# Fractal Dimension Algorithm for Oil Spill and Look-Alike Detections using RADARSAT-1 SAR and AIRSAR/POLSAR Data

**Marghany, M.,[1] Cracknell, A. P.,[2] and Hashim, M.,[3]**
Institute of Geospatial Science & Technology (INSTEG), Faculty of Geoinformation Science and Engineering, Universiti Teknologi Malaysia, 81310 UTM, Skudai
Johore Bahru, Malaysia, E-mail: maged@fksg.utm.my[1], magedupm@hotmail.com[1], mazlan@fksg.utm.my[3], cracknellarthur@hotmail.com[2]

**Abstract**
*Automatic detection of oil spill and look-alikes in synthetic aperture radar (SAR) is required standard procedures. In fact, oil spill and look-alike are appeared as dark patches in SAR data. This work utilizes a modification of the formula of the fractal box counting dimension in which divided a convoluted line of slick embedded in SAR data into small boxes. The method is based on the utilization of the probability distribution formula in the fractal box count. The purpose of this method is to use it for the discrimination of oil spill areas from the surrounding features e.g., sea surface and look-alikes in SAR data i.e., RADARSAT-1 SAR S2 mode and AIRSAR/POLSAR data The results show that the modified formula of the fractal box counting dimension is able to discriminate between oil spills and look-alike areas. The low wind area has the highest fractal dimension peak of 2.9, as compared to the oil slick and the surrounding rough sea. Further, modified formula of fractal box counting dimension is also able to detect look-alikes and low wind zone areas in AIRSAR/POLSAR data. It is interesting to find out that oil spill is absent in AIRSAR/POLSAR data. Both SAR data have maximum error standard deviation of 0.45 which performs with fractal dimension value of 2.9. In conclusion, modification formula of fractal box counting dimension is promising method for oil spill automatic detection in different sensor of SAR data.*

## 1. Review Literature

The synthetic aperture radar (SAR) has been recognized as a powerful tool for oil spill detection. Several algorithms have been introduced for the automatic detection of oil spills in SAR images (Bern et al., 1993, Benelli and Garzelli, 1998 and Aiazzi et al., 2001). These algorithms have involved three steps: (i) dark spot detection, (ii) dark spot feature extraction, and (iii) dark spot classifications. Various classification algorithms for oil spill detection have been utilized, including pattern recognition algorithms (Fukunaga, 1990), spatial frequency spectrum gradient (Lombardini et al., 1989 and Trivero et al., 1998) and fuzzy and neural networks techniques (Mohamed et al. 1999; Calaberesi et al., 1999). Dark spot detection is done by adaptive thresholding. This step is controlled by wind conditions and the type of SAR sensors. However, threshold procedures have failed to detect thin and linear slicks. Available in–situ wind measurements can be used to determine the threshold while the local homogeneity can be used to determine the threshold if there are no in-situ wind measurements. In fact, oil spills detection over SAR images is not at all an easy task. For one thing there are other physical phenomena apart from oil slicks which can also generate dark patches and, for another thing, SAR images are affected by multiplicative noise known as speckle. In this context, dark patches that are not due to oil spills are described as look-alikes. They can be due to low wind speed area, internal waves, biogenic films, grease ice, wind front areas, areas sheltered by land, rain cells, current shear zones, and up-welling zones (Petromar, 1981, Lombardini et al., 1989, Trivero et al., 1998 and Calaberesi et al., 1999). In this context the power-to-mean ratio is considered as a good measurement of texture homogeneity. Utilization of sea surface homogeneity in a SAR image is a function of wind speed conditions. For high or medium wind speeds greater than about 3 m $s^{-1}$ the sea water surrounding dark areas will appear fairly homogenous. This explains the weak possibilities of the presence of oil spill look-alikes in SAR scenes under these conditions. However, with a low wind speed of less than 3 $ms^{-1}$ there could be a large number of oil spill look-alikes presents in SAR imagery (Trivero et al., 1998). The detection of oil spill and look-alike features in SAR scenes can be

obtained by using power-to-mean ratio values. The power-to-mean ratio is used to adjust the threshold. Various authors (Solberg and Solberg, 1996, Solberg and Volden, 1997, Kanna et al., 2003 and Nirchio et al., 2005) have reported that for RADARSAT-1 SAR thresholding is done at three different scales. However, using three different scales did not work well for ENVISAT, due to the larger pixel size of the selected product types. A new approach has been introduced by Maged (2001) to detect thin and linear slicks by using the Lee algorithm (Touzi, 2002). The Lee Filter is primarily used on radar data to remove high frequency speckle without removing edges or sharp features in the images. Maged and van Genderen (2001) reported that the Lee algorithm operates well to determine linear slick features. According to Maged (2001), the Lee algorithm avoids decreasing resolution by making a weighted combination of running average which reduces the noise in the slick's edge areas without sacrificing edge sharpness. Recently, Huang et al., (2005) explored the segmentation of oil slicks using a partial differential equation (PDE)-based level set method with ERS-2 SAR data. They concluded that the level set method allows an extraction of smooth and ideal boundaries rather than a number of zigzag edges. However, this method failed to distinguish between oil slicks and dark spot areas that were located close to the coastline due to low wind speed and were not oil slicks. In fact this method produced automatic snake contours around the presence of any dark spot areas in SAR imagery. Furthermore, Maged and van Genderen (2001) introduced a new approach by using texture algorithms for the automatic detection of oil spills in a RADARSAT-1 SAR image. In fact, grey-tone spatial-dependence or co-occurrence matrices provide the basis for a number of measures including range, variance, standard deviation, entropy, or uniformity within a moving kernel window (Tricot, 1993). This suggests that a large part of the RADARSAT-1 swath could be useful for oil slick detection. Recently, Ivanov et al., (2002) reported that the RADARSAT-1 SAR, in its ScanSAR Narrow mode with swath width that exceeds 300 km, is an attractive tool for marine oil pollution detection. They showed that the entire ScanSAR image can be used for oil slick detection, at least for suitable wind conditions. Further, the standard 2 beam mode is C-band and has a lower signal-to noise ratio due to its HH polarization with wavelength of 5.6 cm and frequency of 5.3 GHz. The RADARSAT-1 SAR standard 2 beam data has spatial resolution of 12.5 m x12.5 m and the swath area of 110 km x 100 km. The incidence angle is between 23.7°and 31.0° (RADARSAT International, 2006). However, computing the texture features from a co-occurrence matrix may become critical due to the multiplicative noise impacts. Different approaches to texture identification have been introduced that involve exploiting the fractal algorithm which can be estimated from a specific multi-resolution representation of the SAR images. Fractal analysis provides tools for measuring how the geometric complexity (the number of discrete objects, perimeter to area ratios, and degree of spatial auto-correlation) of imaged objects changes when the image resolution is altered. The main question that can be raised is how the fractal algorithm can be used to discriminate between oil spills and look-alikes in RADARSAT-1 SAR data. According to Redondo (1996) fractal geometry can be used on occasion to discriminate between different textures. A fractal refers to entities, especially sets of pixels, which display a degree of self-similarity at different scales. Self-similarity is the foundation for fractal analysis and is defined as a property of a curve or surface where each part is indistinguishable from the whole, or where the form of the curve or surface is invariant with respect to scales, meaning that the curve or surface is made of copies of itself at reduced scale and enlarged scales (Pentland, 1984). The most well known procedures that have been proposed for estimating the fractal dimension of SAR images are box counting, fractal Brownian motion (Falconer, 1990, Gado and Redondo, 1999 and Benelli and Garzelli, 1999) and fractal interpolation function system dimension of images (Aiazzi et al., 2001). Initially, Falconer (1990) introduced the fractional Brownian motion model with SAR image intensity variation, which promises in the SAR data textures. In fact, both the sea surface and its backscattered signal in the SAR data can be modeled as fractals (Wornell and Oppenheim, 1992, Maragos and Sun, 1993, Benelli and Garzelli, 1999 and Aiazzi et al., 2001). By contrast, Gado and Redondo (1999) found that a box counting fractal dimension model provided excellent discrimination between oil spills and look-alikes, although the backscatter information, which could allow a first robust localization of the oil spills, had not been considered. Furthermore, Benelli and Garzelli (1999) used a multi-resolution algorithm which was based on fractal geometry for texture analysis. They found that the sea surface is characterized by an approximately steady value of fractal dimension, while the oil spills have a different average fractal dimension compared to look-alikes. This work has hypothesized that the dark spot areas (oil slick or look-alike pixels) and their surrounding backscattered environmental

signals in the SAR data can be modeled as fractals. In this context, a box-counting fractal estimator can be used as a semiautomatic tool to discriminate between oil spills, look-alikes and surrounding sea surface waters. In addition, the utilization of a probability density formula in the box-counting equation can improve the accuracy of discrimination between oil slick pixels and surrounding feature pixels such as ocean surface and look-alikes. The procedures which have been used to discriminate oil spills from the surrounding sea surface environment are shown in Figure 1.

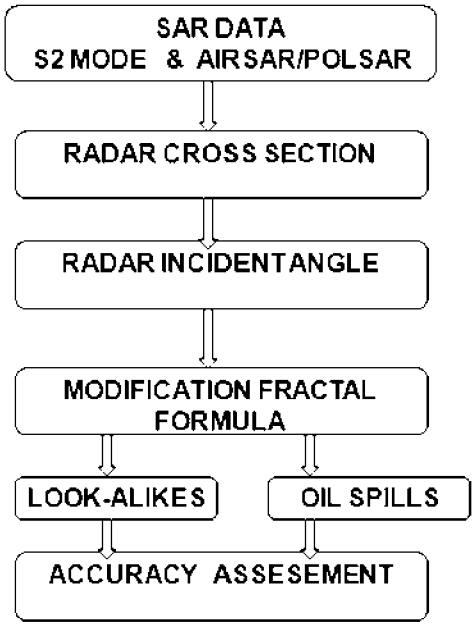


Figure 1: Block diagram of fractal dimension algorithm

## 2. Methodology

*2.1 Data Set*

SAR data acquired in this study were derived from the RADARSAT-1 and AIRSAR/POLSAR images. RADARSAT-1 SAR data that involve Standard beam mode (S2) images. S2 data are C-band and have a lower signal-to noise ratio due to their HH polarization with a wavelength of 5.6 cm and a frequency of 5.3 GHz. Further, S2 data have 3.1 looks and cover an incidence angle of 23.7°and 31.0° (RSI, 2006). In addition, S2 data cover a swath width of 100 km. Both Mohamed et al., (1999) and Hashim et al., (2006) reported the occurrence of oil spill pollution on 20 December 1999, along the coastal water of the Malacca Straits. The Jet Propulsion Laboratory (JPL) airborne Airborne Synthetic Aperture Radar (AIRSAR) data. AIRSARis a NASA/JPL multi-frequency instrument package aboard a DC-8 aircraft and operated by NASA's Ames Research Center at Moffett Field. AIRSAR flies at 8 km over the average terrain height at a velocity of 215 m $s^{-1}$. The system is designed to be flown on small and large aircraft. The system requires a scanner port (18 cm x36 cm) on the aircraft underside. JPL's airborne synthetic aperture radar (AIRSAR) is a unique system, comprising three radars at HH-, VV-, HV- and VH-polarized signals from 5 m x 5 m pixels recorded for three wavelengths: C band (5 cm), L band (24 cm) and P band (68 cm) (Zebker, 1992). AIRSAR data collections are involved; fully polarimetric data (POLSAR) can be collected at all three frequencies, while cross-track interferometric data (TOPSAR) and along-track interferometric (ATI) data can be collected at C- and L-bands.

2.2 *Fractal Algorithm for the Oil Spill Identification*

The oil slick detection tool uses fractal algorithms to detect the self-similar characteristics of RADARSAT-1 SAR and AIRSAR/POLSAR data intensity variations. A box-counting algorithm introduced by Benelli and Garzelli (1999) was used in this study. The box counting algorithm was used to divide a convoluted line of slick which was embedded in both SAR data plane (*i,j*), into smaller boxes. This was done by dividing the initial length of the convoluted line of the slick at backscatter level $\beta_s$ by the recurrence level of the iteration (Gado and Redondo 1999). We define a decreasing sequence of backscattering $\beta_s$ tending from, the largest value, to less than or equal to zero. Following, Gado and Redondo (1999), the fractal dimension $D(\beta_s)$ as a function of the RADARSAT-1 SAR image intensity $\beta_s$ is given by:

$$D(\beta_s) = D_B = \lim_{s\to\infty} \frac{\log M(\beta_s)}{-\log(\beta_s)}$$

Equation 1

Where, $M(\beta_s)$ denotes the number of boxes which are needed to cover the various slick areas with different backscatter intensity $\beta_s$ in both SAR data. In addition, the subscript *s* indicates the backscatter amplitude and its unit is *dB*. The number of boxes was non-overlapping which was calculated from the fractal dimension algorithm and having a square shape with side length $l_s$ unit. This $l_s$ is an odd, positive integer centred on an arbitrary point in the RADARSAT-1 SAR and AIRSAR/POLSAR backscatter images $\beta_s$ surface. Therefore, side length was needed to cover a fractal profile, of

backscatter image $\beta_s^{-D}$, where $D$ is the fractal dimension that is to be estimated. Moreover, the box numbers were chosen based on the length of convoluted line of slick at backscatter level $\beta_s$. If the profile being sampled is a fractal object, then $M(\beta_s)$ should be proportional to $\beta_s^{-D}$, i.e., the following relation, which was adopted from Milan *et al.* (1993), should be satisfied:

$$M(\beta_s) = C\beta_s^{-D}$$

Equation 2

Where $C$ is a positive constant derived from a linear regression analysis between log $M$ ($\beta_s$) and log ($\beta_s$). For different box sizes were needed to cover the length of convoluted line of slick at backscatter level $\beta_s$, a number of points were produced in the log-log plane. The dimension $D$ ($\beta_s$) =$D_B$ can be estimated from a linear regression of these points (Milan et al., 1993). In practice it is difficult to compute $D(\beta_s)$ using equation (1) due to the discrete RADARSAT-1 SAR and AIRSAR/POLSAR data surfaces, and so approximations to this relationship are employed. First, the RADARSAT-1 SAR and AIRSAR/POLSAR intensity images $\beta$ is treated as a two-dimensional matrix $(\beta \times \beta)$. This $\beta \times \beta$ intensity image matrix has been divided into non-overlapping or abutted windows of size $l \times l$, where $l$ is the length of the convoluted line of the slick in both SAR data $(\beta \times \beta)$. In addition for each window, there is a column of accumulated boxes, each box with size of $l^2{}_s \times l$. The backscatter values $(\beta_0)$ are stored at each intersection of the column $i$ and row $j$ of the various slick areas. Then $l$ is calculated by using the differential box counting proposed by Sarkar and Chaudhuri (1994).

$$\left[\frac{\beta_s}{l}\right] = \left[\frac{\beta}{l_s}\right]$$

Equation 3

Let the minimum and maximum $(\beta_s)$ in the $(i, j)$ window fall in boxes numbered $n$ and $m$. The total number of boxes needed to cover the various slick pixels in the RADARSAT-1 SAR image with the box size $l^2{}_s \times l$ is:

$$M(\beta_s) = \sum_{i,j}^{l} n(\beta_0) - m(\beta_s) + 1$$

Equation 4

Let $P[M(\beta_s), l_s]$ be the probability of the total number of boxes $M(\beta_s)$ with box sizes $l_s$. This probability should be directly proportional to the number of boxes $\sum_{i,j}^{l} n(\beta_0) - m(\beta_s) + 1$ spanned on the $(i, j)$ windows. By using equation (4) the expected number of boxes with size $l_s$ which is needed to cover the slick pixels can be calculated using the following formula:

$$M(\beta_s) = \sum_{i,j} \frac{1}{n} P[M(\beta_s), l_s]$$

Equation 5

According to Fiscella et al., (2000), the probability distribution of the dark area belonging to slick pixels can be calculated using the formula below:

$$P[M(\beta_s)] = [1 + \Pi_n q_n(M(\beta_s)) / p_n(M(\beta_s))]$$

Equation 6

Let $n = \sum_{i,j}^{l} n(\beta_0) - m(\beta_s) + 1$, $q$ and $p$ are the probability distribution functions for look-alike and oil spill pixel areas, respectively. From equations (5), (6) and (1) one can get a new formula for estimating the fractal dimension $D_B$

$$D(\beta_s) = D_B = \lim_{\varepsilon \to \infty} \frac{\log \sum_{i,j} n^{-1}[1 + \Pi_n q_n(M(\beta_s)) / p_n(M(\beta_s))]}{-\log(\beta_s)}$$

Equation 7

Equation 7 represents the modification formula of equation 1. In practice, the limit of $M$ going to zero cannot be taken as it does not produce a texture image for oil spills or look-alikes in SAR data. Using fractal dimensions to quantize texture for segmentation, we may divide the slick's pixel areas into overlapping sub-images. Each sub-image is centre on the pixel of interest. We then estimate the fractal dimension $D(\beta_s)$ within each sub-image, and assign the fractal dimension value to the central pixel of each sub-image. This will produce a texture image that may be used as an additional feature in slick pixel classification.

### 3. Results and Discussion

The new fractal formula was trained on three SAR data, whereas the dark spots were identified and examined.

The RADARSAT-1 SAR S2 mode image contained the confirmed oil spills that occurred 20 December 1999 (Samad and Shattri, 2002) (Figure 2a). S2 mode data covered an area located in between 101° 01' 01.01" E to 101° 17' 11.5" E and 2° 25' 38.6" N to 2° 34' 23.5" N The validation of new fractal formula was examined on pairs of AIRSAR/POLSAR data, which were acquired on 6 December 1996 from the coastline of Kuala Terengganu, Malaysia between 103° 5' E to 103° 9' E and 5° 20' N to 5° 27' N. The POLSAR data was acquired on 19 September 2000 from 5°11' N to 5° 12' N and 103' 12' E to 103° 13' E along the southern of Kuala Terengganu, Merang port. (Figures 2b and 2c) (Hashim et al., 2006). Figure 3 shows the variation of the average backscatter intensity along the azimuth direction in the oil-covered areas as a function of incidence angles for the S2 modes. The backscattered intensity was damped -10 dB to -18 dB in S2 (Figure 3). However, both AIRSAR/POLSAR data had higher backscatter intensities as compared to S2 mode data (Figure 3). Further, S2 and AIRSAR/POLSAR data backscatter intensities were well above noise floor value of nominally –20 dB. In fact, RADARSAT-1 SAR is a C-band instrument with a variable acquisition swath, presenting a large variety of possible incidence angles, swath widths, and resolutions (RADARSAT International, 2006). Oil slicks can be detected with a contrast as small as 4 dB (Kotova et al., 1998, Farahiday et al., 1998, and Lu et al., 2000). This suggests that a large part of the RADARSAT-1 swath could be useful for oil slick detection. Nevertheless, Ivanov et al., (2002) reported that the RADARSAT-1 SAR, in its ScanSAR Narrow mode with swath width above 300 km, was attractive for marine oil pollution detection. The wind speed conditions acquired from the Malaysian Meteorological Survey Department showed a maximum offshore wind velocity of 4 m/s during the AIRSAR/POLSAR data overpass and 6.4 and the acquisition of S2 mode data, respectively (Figure 3).

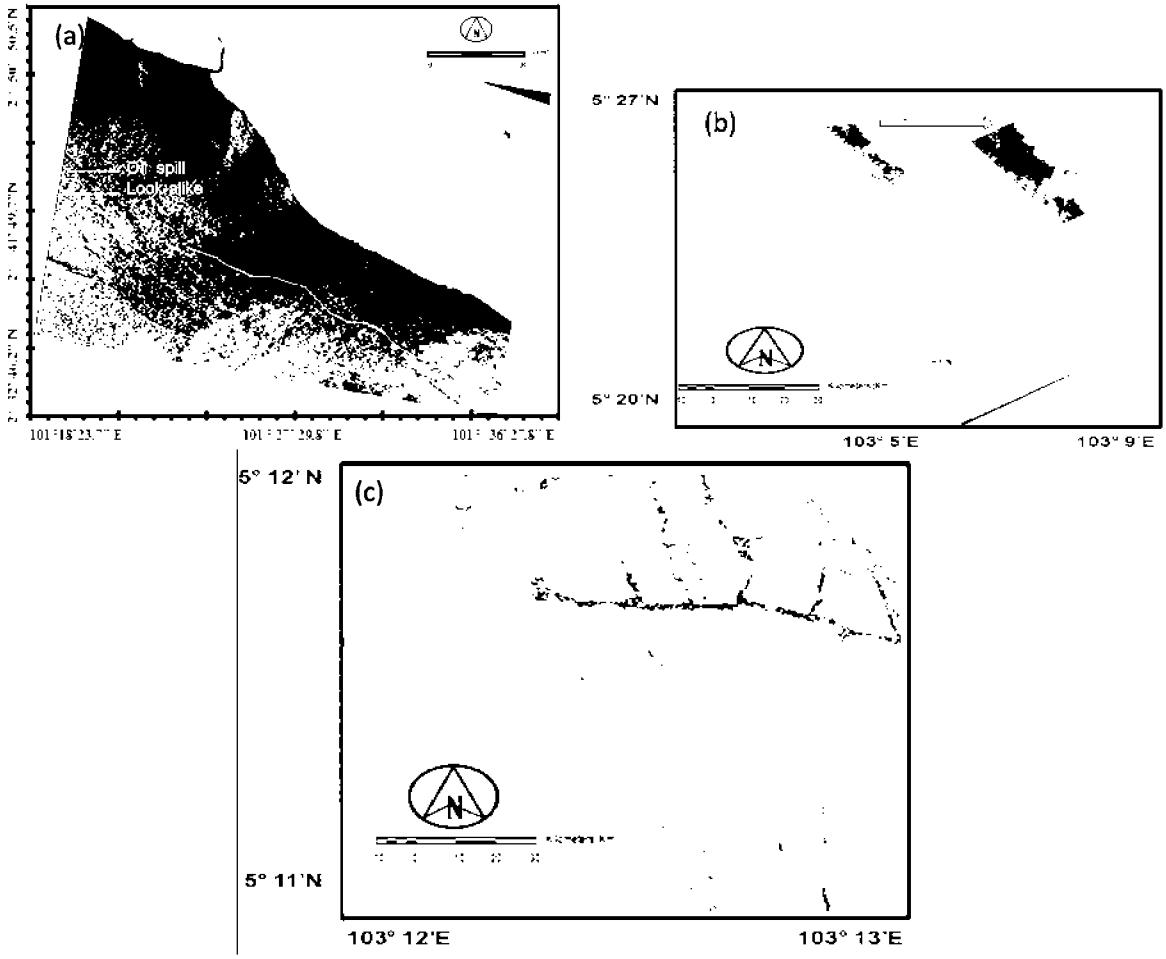


Figure 2: Suspected oil spill in (a) RADARSAT-1 SAR S2 mode data and loo-alikes at (b) AIRSAR data and (c) POLSAR data

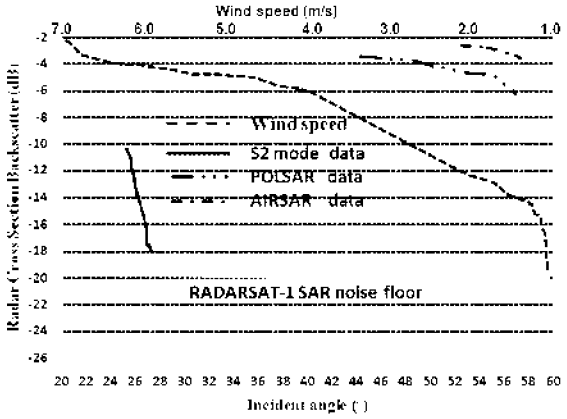


Figure 3: Radar cross section intensity along dark spots in SAR data

In addition, the oil spill in the S2 mode with shallower incidence angle was between 23° and 27° (Figure 3), whereas in the AIRSAR/POLSAR data the dark spots were imaged by steeper incidence angles between 40° and 60° (Figure 3). According to Maged and Mazlan (2005), steeper incidence angles are preferred for oil spill detection, since they tend to maximise the signal from the ocean surface. Our results of backscatter variations across oil spill locations agreed with the study of Maged and Mazlan (2005). The proposed method to estimate the fractal dimension was applied to the amplitude RADARSAT-1 SAR data, by using a 10 x 10 block (Figure 4).

The fractal dimension maps showed a good discrimination between different textures on the RADARSAT-1 SAR image and correlated well with image texture regions. This could be clearly noticed at area (H) where the ship and wake were well identified (Figure 4). The oil spill pixels were dominated by lower fractal values than look-alikes and surrounding environment (Figure 4a). In Figure 4a, the fractal values of oil spill regions varied between 1.49 and 2. According to Maged and Mazlan (2005), the oil spill becomes thinner when the fractal dimension value increases. This could be noticed in areas A to C. In AIRSAR/POLSAR, however, oil spill is absent (Figures 4b and 4c). In fact, a thick oil spill dampens the small-scale waves and therefore there is no Bragg resonance, which reduces the roughness of sea surface as compared to a thin oil spill (Bern et al., 1993). In this context, the fractal dimension is a function of sea surface level intensities over the RADARSAT-1 SAR images, which express the self-similarity (Benelli and Garzelli, 1999). In contrast to the S2 mode data, the fractal dimension values of look-alikes in AIRSAR/POLSAR data were higher. In the AIRSAR/POLSAR, areas F and E represented the occurrence of look-alikes. Table 1 shows that areas E and F in the POLSAR data corresponded to fractal dimension values 2.6 and 2.8, respectively, whereas area E corresponded to a fractal dimension equal to 2.6 in S2 mode data.

Table 1: Fractal values for different features in RADARSAT-1 Standard (S2) mode and POLSAR/AIRSAR data

| AIRSAR/POLSAR | | RADARSAT-1 SAR (S2) | |
|---|---|---|---|
| Area | Fractal dimension | Area | Fractal dimension |
| Oil Spill | | Oil Spill | |
| A | Not exist | A | 1.49 |
| B | | B | 1.52 |
| C | | C | 2.00 |
| Look-alike | | Look –alike | |
| D | - | D | 2.4 |
| E | 2.6 | E | 2.6 |
| F | 2.8 | F | 3.0 |
| Ship | | ship | |
| G | 4.0 | G | 4.0 |
| H | 3.6 | H | 2.4 |
| I | - | I | 3.9 |
| Shear Current | | Shear Current | |
| J | Not exist | J | 3.8 |
| K | | K | 3.9 |
| L | | L | 3.9 |
| Low wind zone | | Low wind zone | |
| M | 1.56 | M | 1.57 |
| N | 2.21 | N | 2.00 |
| O | 2.52 | O | 2.48 |

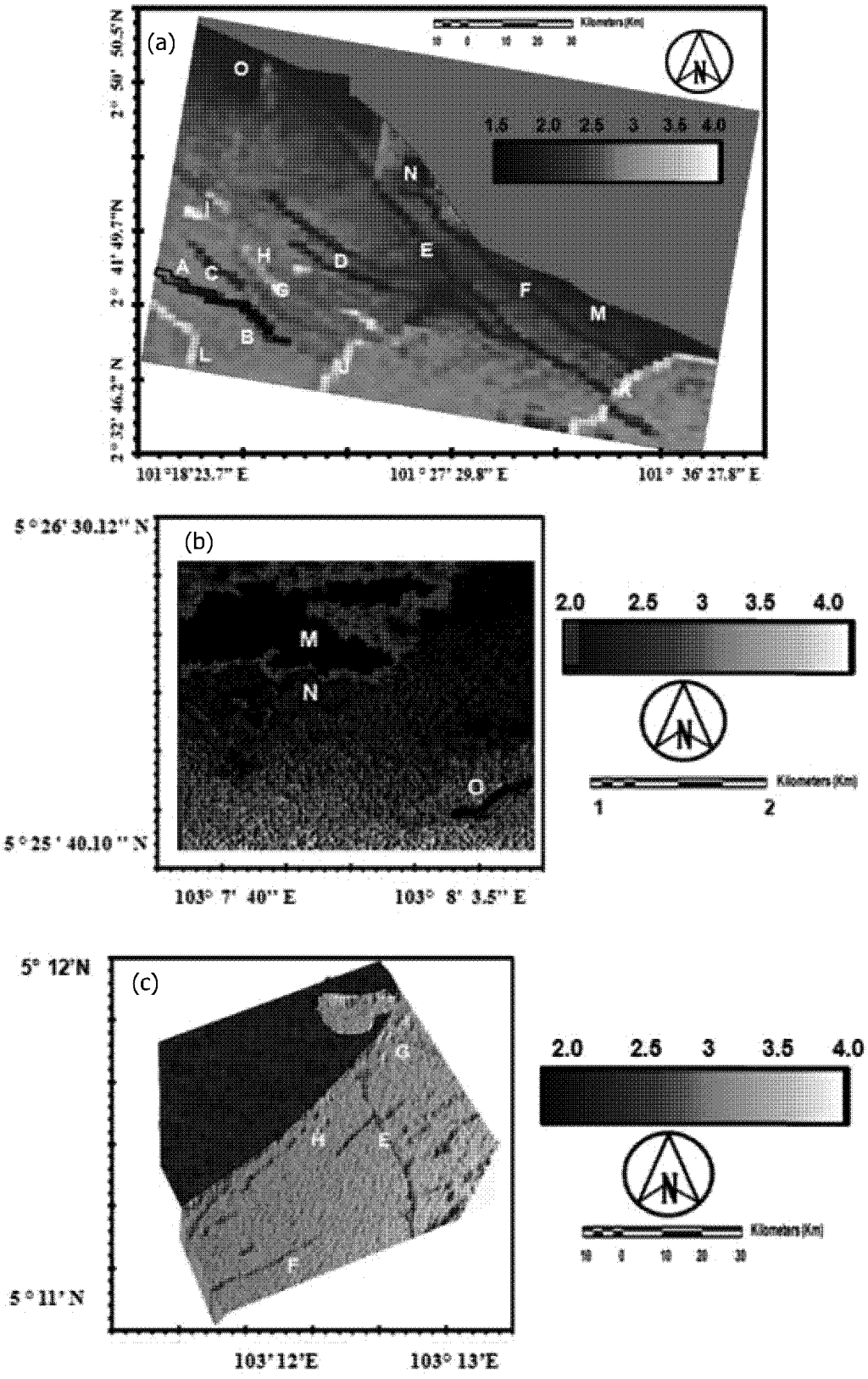


Figure 4: Fractal map for (a) RADARSAT-1 SAR S2 mode data, (b) AIRSAR and (c) POLSAR

Figures 4a and 4c show the highest fractal dimension values of 3.9 and 4.0 in areas I and G, respectively, were represented by the presence of a ship, whereas ship waves had a lower fractal dimension values, between 2.4 and 3.6 in area H in AIRSAR/POLSAR and S2 mode data, respectively (Table 1). Furthermore, the occurrence of shear current flow could be seen in areas J, K and L, respectively in S2 mode data (Figure 4a). It was interesting to find that the fractal dimension algorithm-based probability was able to extract ship wake information in area H with a value of 3.9 (Figure 4a). This suggests that the corresponding value of fractal dimension for different categories allows a multi-fractal characterisation of different features in different SAR data. These results confirmed the study of Maged and Mazlan (2005).

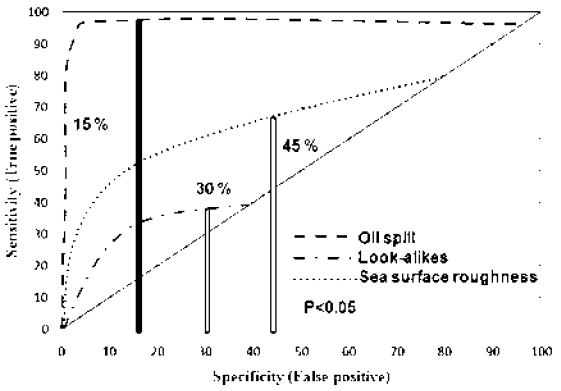


Figure 5: ROC Curve for different feature detection in SAR data

In AIRSAR/POLSAR and S2 mode data, it could further be seen that low wind zones in areas M, N and O occurred close to the coastline, with maximum fractal values equal to 2.33, 2.34 and 2.5, respectively (Figure 6). Look-alikes occupied narrow areas parallel to the coastline (Figure 6). The wide distribution of dark zone pixels represented the natural slick in low wind areas (Henschel et al., 1997), which was aligned with what could be a current shear or convergence zone. This could be seen clearly in S1 mode data (Figure 6a). Thus, the fractal algorithm was able to discriminate the look-alike features from the surrounding sea surface features such as current shear (Figure 6a). Figure 6b illustrates, however, larger areas of look-alikes as compared to Figure 6a.

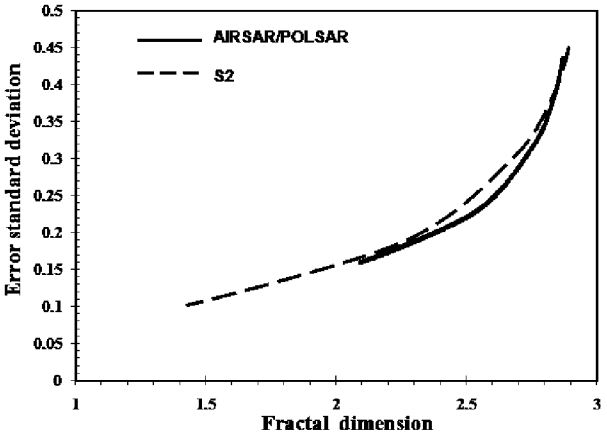


Figure 6: Accuracy assessment of fractal dimension performance

The fractal dimension values of look-alikes and ships and shown in Figures 4a, 4b and 4c were approximately similar. The receiver-operator-characteristics (ROC) Curve in Figure 5 indicates significant differences in the discrimination between oil spill, look-alikes and sea surface roughness pixels. In terms of ROC area, this evidence was provided by an area difference of 15% for oil spill and 45% for the sea roughness and a $p$ value below 0.005, which confirms the study of Maged and Mazlan (2005). In fact, the fractal dimension could be viewed as a measure of the scale of the self-similarity of the object. Also, the interference was statistically similar if the scale was reduced, similar to the result of Bertacca et al., (2005). This suggsts that a fractal analysis is a good method to discriminate regions of oil slick from surrounding water features. Figure 6 shows an exponential relationship between fractal dimension and the standard deviation of the estimation error for the fractal dimension. The maximum error standard deviation was 0.27, corresponding to the fractal dimension value of 2.9, which was found in S2 mode data. For oil spill detection, the minimum error standard deviation of 0.02 occurred in a region of fractal dimension of 1.49 in S2 mode data. For AIRSAR/POLSAR data, the maximum error standard deviation is 0.4 which corresponds to the fractal dimension value of 2.8. This means that the S2 mode performed better for detection of oil spills. In fact, the S2 mode showed a shallower incident angle than AIRSAR/POLSAR data. Wind speeds below 6 m/s are appropriate for detection of oil spills in SAR data (Solberg and Volden, 1997). Therefore, for applications that require imaging of the ocean surface, steep incidence angles are preferable as there is a greater contrast of backscatter manifested at the ocean surface. A good discrimination between oil spill, look-alike, low wind zone and sea surface roughness exists when the error standard deviation is between 0.002 and 0.45, as produced by implementation of the fractal

modified formula. The reason is that the fractal dimension is a measure of the scale of the self-similarity of the object. The low standard deviation error value of 0.002 for fractal areas of 1.49 dominate by the oil spill was lower than that for the surrounding sea. This is an excellent indicator for the validation of the fractal formula modification by implementing a probability distribution function (PDF). The fractal dimension based on the probability distribution function (PDF) improves the discrimination between oil spill, look-alikes, sea roughness and low wind zones. In fact, involving the PDF formula in the fractal dimension map directly relates the textures at different scales to the fractal dimension. Such a modification of the fractal equation reduces the problems of speckle and sea clutter and assists in the accurate classification of different textures for SAR images. Previous studies were concerned with automatic detection of oil spills from SAR images, which is based on dark spot feature extraction and classification (Solberg and Solberg, 1996, Solberg and Volden, 1997, Benelli and Garzelli, 1999, Mohamed et al., 1999, Samad and Shattri, 2002 and Maged and Mazlan, 2005). In contrast to the present study, those studies failed to detect the oil spill spreading and to discriminate between the current shear features, ship pixels, sea surface roughness and oil spill pixels by using different segmentation algorithms (Solberg and Solberg, 1996, Solberg and Volden, 1997, Mohamed et al., 1999 and Samad and Shattri, 2002) or the classical fractal formula (Benelli and Garzelli, 1999 and Maged and Mazlan, 2005). Indeed, the different oil spill segmentation approaches, in terms of accuracy of classification of oil spills and features of the surrounding sea, are a challenging task; the modification of the algorithms used for automatic detection of oil spills might be required to improve the analyses.

## 4. Conclusion

The utilization of multi SAR imagery for oil slick detection has been implemented by using a fractal dimension algorithm as an automatic tool to discriminate between an oil slick and other surface features such as slick look-alikes and variability of surface roughness. The oil spill has characteristic values of fractal dimension, which ranged between 1.49 and 2.0. The sea surface roughness has a steady value of fractal dimension which is 2.6. The interesting result is that the low wind area was characterised by the highest value of fractal dimension which is 2.48. In AIRSAR/POLSAR data, the look-alike due to natural slick has characteristic values of fractal dimension, which ranged between 1.6 and 2.0. The sea surface roughness has a steady value of fractal dimension which is 2.4. The interesting result is that the ship pixels were characterised by the highest value of fractal dimension which is 3.9. The maximum error standard deviation of 0.45 which performs with fractal dimension value of 2.9 is found in both SAR data. It can be said that the new approach of the fractal box counting dimension algorithm can be used as an automatic tool for oil spill, and look-alike detections in different sensor of SAR data.

## References


Aiazzi, B., Alparone, L., Baronti, S., and Garzelli, A., 2001, Multiresolution Estimation of Fractal Dimension from Noisy Images". *SPIE-IS&T Journal of Electronic Imaging*, 10, 339-348.

Benelli, G., and Garzelli, A., 1998, A Multi-Resolution Approach to Oil-Spills Detection in ERS-1 SAR Images. *Image and Signal Processing for Remote Sensing*, 145-156.

Benelli, G., and Garzelli, A., 1999, Oil-spill detection in SAR images by fractal dimension Estimation. . In *Proceedings of* Geosciences and Remote Sensing Symposium, 1999, *IGARSS'99, Hamburg, Germany, 28 June-2 July 1999, IEEE Geoscience and Remote Sensing Society, USA.* Vol. 2, 1123-1126.

Bern, T. I., Wahl, T., Anderssen, T., and Olsen, R., 1993, Oil Spill Detection Using Satellite Based SAR; Experience from a Field Experiment". *Photogrammetric Engineering and Remote Sensing*, 59, 423-428.

Bertacca, M., Berizzi, F., and Mese, E. D., 2005, A FARIMA-Based Technique for Oil Slick and Low-Wind Areas Discrimination in Sea SAR Imagery. *IEEE Transactions on Geosciences and Remote Sensing*, 43, 2484-2439.

Calaberesi, G., Del Frate, F., Lightenegger, J., Petrocchi, A., and Trivero, P., 1999, Neural Networks for the Oil Spill Detection using ERS-SAR Data. In Proceedings *of* Geosciences and Remote Sensing Symposium, 1999, *IGARSS'99*, Hamburg, Germany, 28 June-2 July 1999, *IEEE Geosciences and Remote Sensing Society, USA.* Vol. 1, 215-217.

Farahiday, I., Suryono, G. F., and Arvelyna, Y., 1998, Utilization of RADARSAT SAR Data for Oil Slick Detection and Vessel Ship Monitoring Application: ADRO 630 Projects. *GIS and Remote Sensing Year Book,* Academic Press, New York, BPPT 97/98.

Fiscella, B., Giancaspro, A., Nirchio, F., Pavese, P., and Trivero, P., 2000, Oil Spill Detecting using Marine SAR images. *International Journal of Remote Sensing*. Vol. 12, No. 18, 3561-3566.

Falconer, K., 1990, *Fractal geometry*, John Wiley & Sons, New York.

Fukunaga, K., 1990, *Introduction to Statistical Pattern Recognition*. 2nd edition, Academic Press, New York.

Gade, M., and Redondo, J. M., 1999, Marine Pollution in European Coastal Waters Monitored by the ERS-2 SAR: A Comprehensive Statistical Analysis. In Proceedings of Geosciences and Remote Sensing Symposium, 1999, IGARSS'99, Hamburg, Germany, 28 June-2 July *1999, IEEE Geosciences and Remote Sensing Society,* USA. Vol. 2, 1375–1377.

Henschel, M. H., Olsen, R. B., Hoyt, P., and Vachon, P. W., 1997, The Ocean Monitoring Workstation: Experience Gained with RADARSAT. *Proceedings of Geomatics in the Era of RADARSAT*, Canadian Center of Remote Sensing, Canada, 25-30 May 1997, Ottawa, Canada. Canadian Center of Remote Sensing, Ottawa. CD-ROM Proceedings (1997).

Huang, B., Li, H., Huang, X., 2005, A level Set Method for Oil Slick Segmentation in SAR Images, *International Journal of Remote Sensing*, 26, 1145-1156.

Ivanov, A., He, M., and Fang, M. Q., 2002, Oil Spill Detection with the RADARSAT SAR in the Waters of the Yellow and East Sea: A case study CD *of 23rd Asian Conference on Remote Sensing*, 13-17 November 2002, Nepal, Asian Remote Sensing Society, Japan. Vol. 1, 1-8.

Kanna, T., Tonye, E., Mercier, G., Onana, V. P., Ngono, J. M., Frison, P. L., Rudant, J. P. and Garello, R., 2003., Detection of Oil Slick Signatures in SAR Images by Fusion of Hysteresis Thresholding Responses. *In Proceedings of Geosciences and Remote Sensing Symposium*, 2003, IGARSS'03, Toulous, France, 8 June-12 June 2003, IEEE Geosciences and Remote Sensing Society, USA. Vol. 3, 2750–2752.

Kotova, L., Espedal, H. A., and Johannessen, O. M., 1998, Oil Spill Detection using Spaceborne SAR: A Brief Review". *Proceedings of 27th International Symposium on Remote Sensing Environmental*, 8-12 June 1998, Norwegian Defence Research Establishment. Tromsø, Norway, 791-794.

Lombardini, P. P., Fiscella, B., Trivero, P., Cappa, C., and Garrett, W. D., 1989, Modulation of the Spectra of Short Gravity Waves by Sea Surface Films: Slick Detection and Characterization with Microwave Probe. *Journal of Atmospheric and Oceanic Technology*, 6, 882-890.

Lu, J., Kwoh, L. K., and Lim, H., 2000, Mapping Oil Pollution from Space", *Backscatter*, February, 23-26.

Maragos, P. and Sun, F. K., 1993, Measuring the Fractal Dimension of Signals: Morphological Covers and Iterative Optimization. *IEEE Transactions Signal Processing*, 41,108–121.

Maged, M., 2001, RADARSAT Automatic Algorithms for Detecting Coastal Oil Spill Pollution. *International Journal of Applied Earth Observation and Geoinformation*, 3, 191-196.

Maged, M., and van Genderen, J., 2001, Texture Algorithms for Oil Pollution Detection and Tidal Current Effects on Oil Spill Spreading. *Asian Journal of Geoinformatics,* 1, 33-44.

Maged, M., and H., Mazlan, 2005, Simulation of Oil Slick Trajectory Movements from the RADARSAT-1 SAR. *Asian Journal of Geoinformatics,* 5, 17-27.

Mohamed, I. S., Salleh, A. M., and Tze, L. C., 1999, Detection of Oil Spills in Malaysian Waters from RADARSAT Synthetic Aperture Radar Data and Prediction of Oil Spill Movement. *Proceeding of 19th Asian Conference on Remote Sensing,* China, Hong Kong, 23- 27 November 1999, Asian Remote Sensing Society, Japan, Vol. 2, 980-987.

Milan, S., Vachav, H., and Roger, B., 1993, *Image Processing Analysis and Machine Vision.* Chapman and Hall Computing, New York.

Nirchio, F., Sorgente, M., Giancastro, A., Biaminos, W., Parisatos, E., Raveras, R., Trivero, P., 2005, Automatic Detection of Oil Spill from SAR Images. *International Journal of Remote Sensing*, 26, 1157-1174.

Petromar, 1981, Petroleum and the Marine Environment. Graham and Trotman, London.

Pentland,A.P., (1984) Fractal-based description of natural scenes. *IEEE Transactions Pattern Analysis and Machine Intelligent.* 6, 661-674, 1984.

Redondo, J. M., 1996, Fractal Description of Density Interfaces. *Journal of Mathematics and its Applications.* 5, 210-218.

RADARSAT International, 2006, RADARSAT Applications (*http:\www.rsi.ca\March 3, 2006).*

Samad, R., and Mansor, S. B., 2002, Detection of Oil spill Pollution using RADARSAT SAR Imagery. http://www.gisdevelopment.net /aars/acrs/2002/sar/096.pdf.

Sarkar, N., and Chaudhuri, B. B., 1994, An efficient Differential Box-counting Approach to Compute Fractal Dimension of Image. *IEEE Transactions Systems,* Man. Cyber-net. 24, 115-120

Solberg, A. H. S., and Solberg, R., 1996, A large-scale evaluation of features for automatic detection of oil spills in ERS SAR images. In *International Geosciences and Remote Sensing Symposium'96,*27-31,May 1996, Lincoln, Nebraska, , *IEEE Geosciences and Remote Sensing Society* , USA. Vol. 3, 1484-1486.

Solberg, A. H. S., Volden, E., 1997, Incorporarion of Prior Knowledge in Automatic Classification of Oil Spills in ERS SAR Images. In International Geosciences and Remote Sensing Symposium'97, 3-8 Aug.1997, Singapore, *IEEE Geoscience and Remote Sensing Society,* USA. Vol. 1, 157-159.

Teivero, P., Fiscella, B.,Gomez, F., and Pavese, P., 1998, SAR Detection and Characterisation of Sea Surface Slicks. *International Journal of Remote Sensing,* 19,543-548.

Tricot, C., 1993, *Curves and Fractal Dimension*, Springer Verlag.

Touzi, R., 2002, A review of Speckle Filtering in the Context of Estimation Theory, *IEEE Transactions on Geoscience and Remote Sensing,* 40, 2392 – 2404.

Wornell, G. W., and Oppenheim, A., 1992, Estimation of Fractal Signals from Noisy Measurements using Wavelets," *IEEE Transactions Signal Processing*, 40, 611–623.

Zebker, H. A., 1992, The TOPSAR Interferometric Radar Topographic Mapping Instrument. *IEEE Transactions on Geosciences and Remote Sensing*, 30, 933-940.